Eychenne, J., and S.L. Engwell, 2022, The grainsize of volcanic fall deposits: Spatial trends and physical controls: GSA Bulletin, https://doi.org/10.1130/B36275.1.

Supplemental Material

Figure S1. Example of downwind variations in grainsize in tephra fall deposits from the 18 May 1980 Mount St Helens eruption.

Figure S2. Variations in Md from bulk GSDs vs. deconvolved GSDs with distance from vent, for 4 tephra fall deposits showing polymodal grainsize distributions.

Figure S3. Coarse, fine and distal unimodal grainsize trends represented by variations of Md with distance from vent, for each of the fallout deposits within our dataset (Table 1 and S2) ordered according to plume height.

Table S1. Median Diameter (Md in mm) of the grainsize distributions at individual locations for the 56 tephra fall deposits compiled in our dataset (Table 1)

Table S2. Expanded information list for the 57 tephra fall deposits compiled in this work, showing information on the deposits, eruptions, and grainsize measurement methods.

Table S3. Summary of the statistical information of the Md distributions at given distance intervals from vent as a function of style, plume height above vent and magnitude (data illustrated in Fig. 4 and Fig. S4).

List of the references listed in Table 1 in the main text

Supplemental Figures:

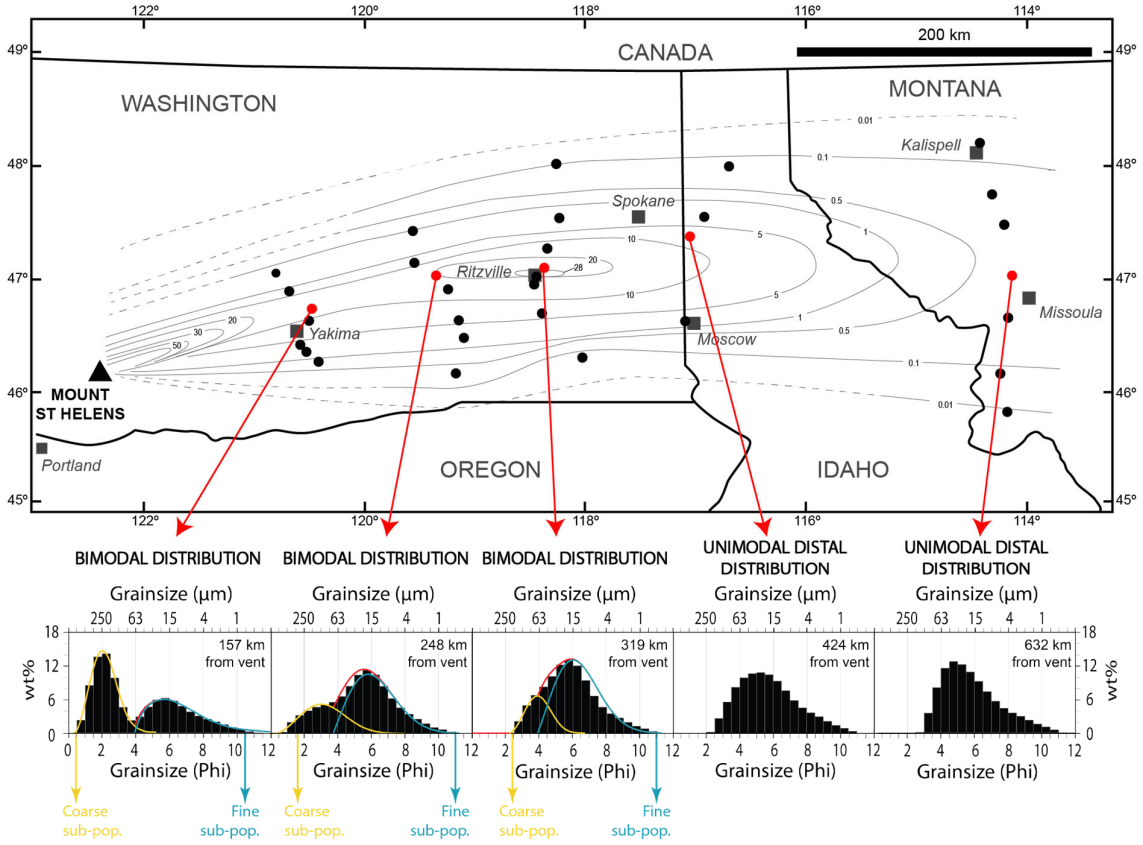

Fig. S1: Example of downwind variations in grainsize in tephra fall deposits from the 18 May 1980 Mount St Helens eruption. The grainsize distributions are bimodal until about 300 km from vent, with a coarse subpopulation shifting towards the fine subpopulation, which then become impossible to distinguish in distal grainsize distributions which are unimodal with a fines-rich tail. Coarse and fine subpopulations are obtained by deconvolution of the bulk grainsize distribution.

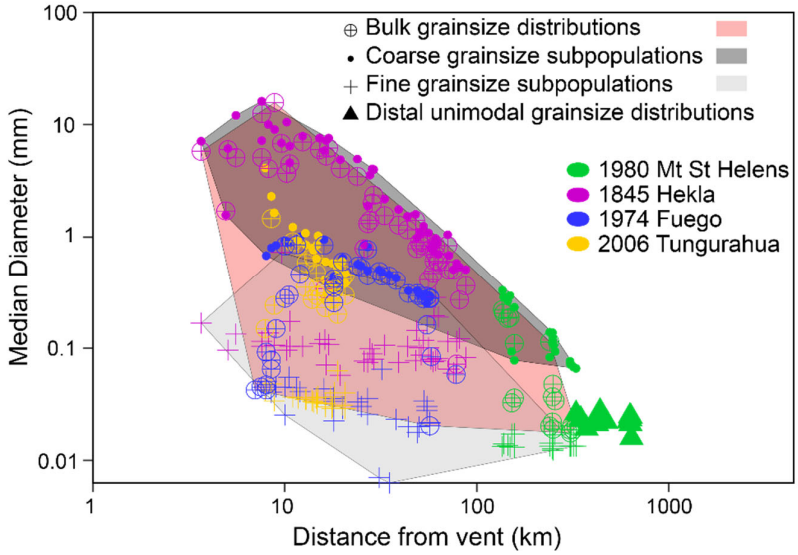

Fig. S2: Variations in Md from bulk GSDs vs. deconvolved GSDs with distance from vent, for 4 tephra fall deposits showing polymodal grainsize distributions (see Table 1 and S2 for eruption characteristics and deconvolution method). Deconvolved GSDs are represented by coarse and fine subpopulations. The red, grey and light grey shaded areas represent the fields covered by the bulk GSDs, the coarse subpopulations and the fine subpopulations, respectively.

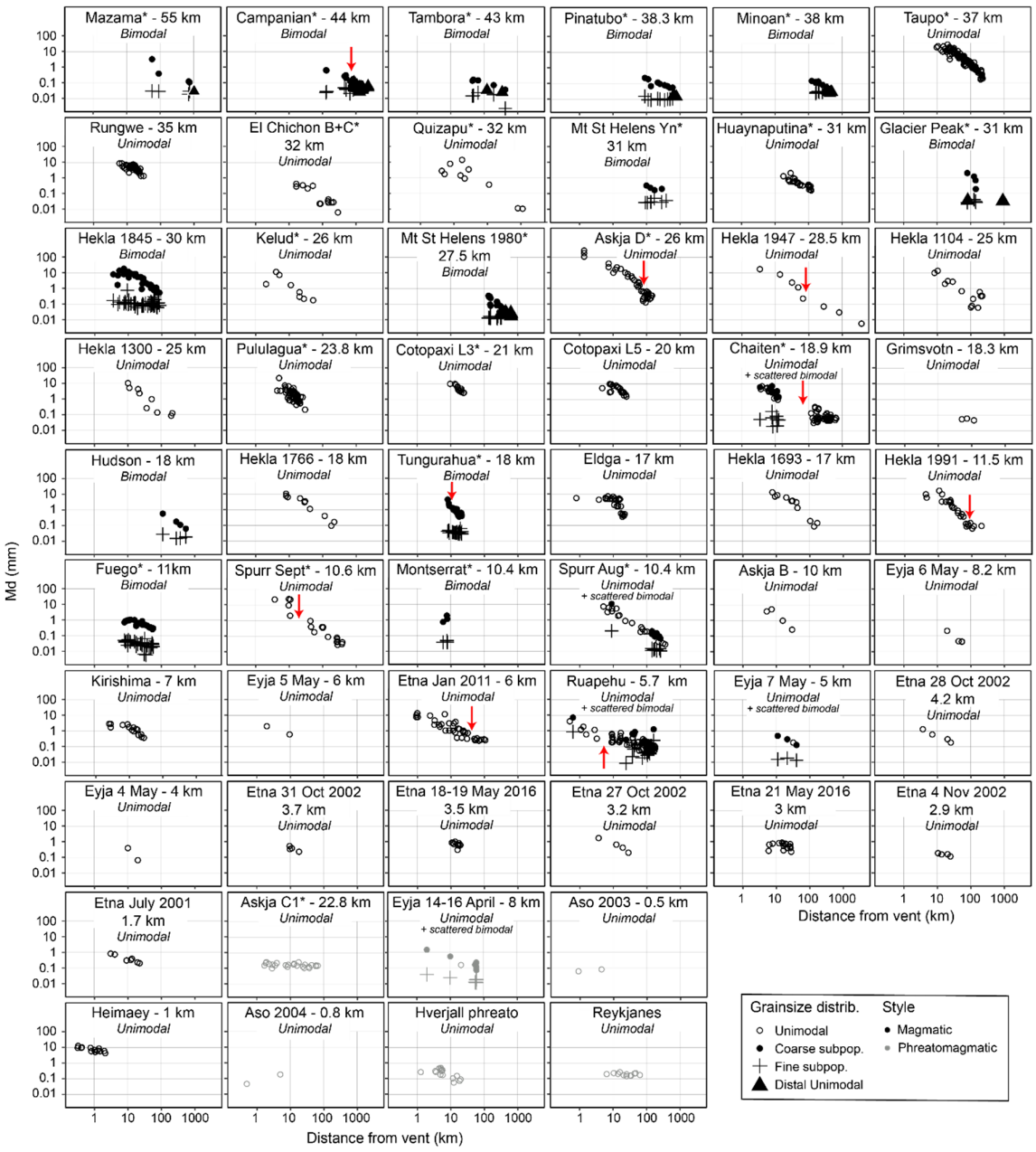

Fig. S3: Coarse, fine and distal unimodal grainsize trends represented by variations of Md with distance from vent, for each of the fallout deposits within our dataset (Table 1 and S2) ordered according to plume height (largest to smallest). Asterix denote those eruptions with pyroclastic density currents. Red arrows indicate break-in-slopes in the grainsize decay trends with distance.

Supplemental Tables:

Table S1: Median Diameter (Md in mm) of the grainsize distributions at individual locations for the 56 tephra fall deposits compiled in our dataset (Table 1)
→ *Provided as an excel spreadsheet in the repository*

Table S2: Expanded information list for the 57 tephra fall deposits compiled in this work, showing information on the deposits, eruptions, and grainsize measurement methods.
→ *Provided as an excel spreadsheet in the repository*

Table S3: Summary of the statistical information of the Md distributions at given distance intervals from vent as a function of style, plume height above vent and magnitude (data illustrated in Fig. 4 and Fig. S4).
→ *Provided as an excel spreadsheet in the repository*

References listed in Table 1 in the main text:

1. Liu, E.J., et al., Contrasting mechanisms of magma fragmentation during coeval magmatic and hydromagmatic activity: the Hverfjall Fires fissure eruption, Iceland. Bulletin of Volcanology, 2017. 79(10): p. 68.
2. Walker, G.P.L., The Taupo pumice: Product of the most powerful known (ultraplinian) eruption? Journal of Volcanology and Geothermal Research, 1980. 8(1): p. 69-94.
3. Pyle, D.M., The thickness, volume and grainsize of tephra fall deposits. Bulletin of Volcanology, 1989. 51: p. 1-15.
4. Houghton, B.F., R.J. Carey, and M.D. Rosenberg, The 1800a Taupo eruption: "III wind" blows the ultraplinian type event down to Plinian. Geology, 2014. 42(5): p. 459-461.
5. Fontijn, K., et al., The ~4-ka Rungwe Pumice (South-Western Tanzania): a wind-still Plinian eruption. Bulletin of Volcanology, 2011. 73(9): p. 1353-1368.
6. Adams, N.K., et al., The physical volcanology of the 1600 eruption of Huaynaputina, southern Peru. Bulletin of Volcanology, 2001. 62(8): p. 493-518.
7. Prival, J.M., et al., New insights into eruption source parameters of the 1600 CE Huaynaputina Plinian eruption, Peru. Bulletin of Volcanology, 2019. 82(1): p. 7.
8. Hildreth, W. and R.E. Drake, Volcan Quizapu, Chilean Andes. Bull Volcanol, 1992. 54: p. 63-125.
9. Rose, W. and A. Durant, El Chichon volcano, 4 April 1982: Volcanic cloud history and fine ash fallout. Nat Haz, 2009. 51: p. 363 - 374.
10. Carey, S. and H. Sigurdsson, The 1982 eruptions of El Chichon volcano, Mexico (2): Observations and numerical modelling of tephra-fall distribution. Bulletin of Volcanology, 1986. 48: p. 127-141.
11. Thorarinsson, S., The eruption of Hekla, 1947-1948, Part II 3. The tephra-fall from Hekla on March 29 th, 1947. Visindafelag Islendinga, 1954. 68.
12. Sparks, R.S.J., L. Wilson, and H. Sigurdsson, The pyroclastic deposits of the 1875 eruption of Askja, Iceland. Philosophical Transactions of the Royal Society of London. Series A, Mathematical and Physical Sciences, 1981. 299(1447): p. 241-273.
13. Carey, R.J., B.F. Houghton, and T. Thordarson, Tephra dispersal and eruption dynamics of wet and dry phases of the 1875 eruption of Askja Volcano, Iceland. Bulletin of Volcanology, 2010. 72(3): p. 259-278.
14. Maeno, F., et al., A sequence of a plinian eruption preceded by dome destruction at Kelud volcano, Indonesia, on February 13, 2014, revealed from tephra fallout and pyroclastic density current deposits. Journal of Volcanology and Geothermal Research, 2019. 382: p. 24-41.
15. Vernier, J.-P., et al., In situ and space-based observations of the Kelud volcanic plume: The persistence of ash in the lower stratosphere. Journal of Geophysical Research: Atmospheres, 2016. 121(18): p. 11,104-11,118.
16. Janebo, M.H., et al., Total grain-size distribution of four subplinian–Plinian tephras from Hekla volcano, Iceland: Implications for sedimentation dynamics and eruption source parameters. Journal of Volcanology and Geothermal Research, 2018. 357: p. 25-38.
17. Janebo, M.H., et al., Dispersal of key subplinian–Plinian tephras from Hekla volcano, Iceland: implications for eruption source parameters. Bulletin of Volcanology, 2016. 78(10): p. 66.
18. Volentik, A.C.M., et al., Modeling tephra dispersal in absence of wind: Insights from the climactic phase of the 2450BP Plinian eruption of Pululagua volcano (Ecuador). Journal of Volcanology and Geothermal Research, 2010. 193(1): p. 117-136.
19. Tsunematsu, K. and C. Bonadonna, Grain-size features of two large eruptions from Cotopaxi volcano (Ecuador) and implications for the calculation of the total grain-size distribution. Bulletin of Volcanology, 2015. 77(7): p. 64.
20. Biass, S. and C. Bonadonna, A quantitative uncertainty assessment of eruptive parameters derived from tephra deposits: the example of two large eruptions of Cotopaxi volcano, Ecuador. Bulletin of Volcanology, 2011. 73(1): p. 73-90.

21. Liu, E.J., et al., The role of bubbles in generating fine ash during hydromagmatic eruptions. Geology, 2015. 43(3): p. 239-242.
22. Olsson, J., et al., Rapid release of metal salts and nutrients from the 2011 Grímsvötn, Iceland volcanic ash. Geochimica et Cosmochimica Acta, 2013. 123: p. 134-149.
23. Hreinsdóttir, S., et al., Volcanic plume height correlated with magma-pressure change at Grímsvötn Volcano, Iceland. Nature Geoscience, 2014. 7(3): p. 214-218.
24. Petersen, G.N., H. Bjornsson, and P. Arason, The impact of the atmosphere on the Eyjafjallajökull 2010 eruption plume. Journal of Geophysical Research: Atmospheres, 2012. 117(D20).
25. Petersen, G.N., et al., Two weather radar time series of the altitude of the volcanic plume during the May 2011 eruption of Grímsvötn, Iceland. Earth Syst. Sci. Data, 2012. 4(1): p. 121-127.
26. Moreland, W., Explosive activity in flood lava eruptions: A case study of the 10th century eldgjá eruption. Iceland (Ph. D. Thesis), University of Iceland, 2017.
27. Gudnason, J., et al., The opening subplinian phase of the Hekla 1991 eruption: properties of the tephra fall deposit. Bulletin of Volcanology, 2017. 79(5): p. 34.
28. Gudmundsson, A., et al., The 1991 eruption of Hekla, Iceland. Bulletin of Volcanology, 1992. 54(3): p. 238-246.
29. Eychenne, J., et al., Distal Enhanced Sedimentation From Volcanic Plumes: Insights From the Secondary Mass Maxima in the 1992 Mount Spurr Fallout Deposits. Journal of Geophysical Research: Solid Earth, 2017. 122(10): p. 7679-7697.
30. McGimsey, R.G., C.A. Neal, and C.M. Riley, Areal distribution, thickness, mass, volume and grainsize of tephra-fall deposits from the 1992 eruptions of Creater Peak vent, Mt. Spurr Volcano, Alaska. U.S. Geological Survey Open-File Report, 2001. 01-370.
31. Rose, W., A. Kostinski, and L. Kelley, Real-Time C-Band Radar Observations of 1992 Eruption Clouds from Crater Peak, Mount Spurr Volcano, Alaska. The 1992 eruptions of Crater PEak vent, Mount Spurr volcano, Alaska. U.S. Geological Survey Bulletin, 1995. 2139.
32. Gudmundsson, M.T., et al., Ash generation and distribution from the April-May 2010 eruption of Eyjafjallajökull, Iceland. 2012. 2: p. 572.
33. Bonadonna, C., et al., Tephra sedimentation during the 2010 Eyjafjallajökull eruption (Iceland) from deposit, radar, and satellite observations. Journal of Geophysical Research: Solid Earth, 2011. 116(B12): p. B12202.
34. Gislason, S.R., et al., Characterization of Eyjafjallajökull volcanic ash particles and a protocol for rapid risk assessment. Proceedings of the National Academy of Sciences, 2011. 108(18): p. 7307-7312.
35. Gislason, S.R., et al., Volcanic ash from the 2010 Eyjafjallajökull eruption. Applied Geochemistry, 2011. 26: p. S188-S190.
36. Dellino, P., et al., Ash from the Eyjafjallajökull eruption (Iceland): Fragmentation processes and aerodynamic behavior. Journal of Geophysical Research: Solid Earth, 2012. 117(B9): p. n/a-n/a.
37. Miyabuchi, Y., et al., Stratigraphy, grain-size and component characteristics of the 2011 Shinmoedake eruption deposits, Kirishima Volcano, Japan. Journal of Volcanology and Geothermal Research, 2013. 258: p. 31-46.
38. Suzuki, Y.J. and T. Koyaguchi, 3D numerical simulation of volcanic eruption clouds during the 2011 Shinmoe-dake eruptions. Earth, Planets and Space, 2013. 65(6): p. 10.
39. Edwards, M.J., et al., Shallow factors controlling the explosivity of basaltic magmas: The 17–25 May 2016 eruption of Etna Volcano (Italy). Journal of Volcanology and Geothermal Research, 2018. 357: p. 425-436.
40. Andronico, D., et al., The 2002–03 Etna explosive activity: Tephra dispersal and features of the deposits. Journal of Geophysical Research: Solid Earth, 2008. 113(B4): p. n/a-n/a.
41. Andronico, D., et al., Representivity of incompletely sampled fall deposits in estimating eruption source parameters: a test using the 12–13 January 2011 lava fountain deposit from Mt. Etna volcano, Italy. Bulletin of Volcanology, 2014. 76(10): p. 861.
42. Calvari, S., Salerno, G.G., Spampinato, L., Gouhier, M., La Spina, A., Pecora, E., Harris, A.J., Labazuy, P., Biale, E. and Boschi, E., 2011. An unloading foam model to constrain Etna's 11–13 January 2011 lava fountaining episode. Journal of Geophysical Research: Solid Earth, 116(B11).
43. Scollo, S., P. Del Carlo, and M. Coltelli, Tephra fallout of 2001 Etna flank eruption: Analysis of the deposit and plume dispersion. Journal of Volcanology and Geothermal Research, 2007. 160(1): p. 147-164.
44. Self, S., et al., The 1973 Heimaey Strombolian Scoria deposit, Iceland. Geological Magazine, 1974. 111(6): p. 539-548.
45. Miyabuchi, Y., S.-i. Ikebe, and K. Watanabe, Geological constraints on the 2003–2005 ash emissions from the Nakadake crater lake, Aso Volcano, Japan. Journal of Volcanology and Geothermal Research, 2008. 178(2): p. 169-183.
46. Magnúsdóttir, A.O., Characteristics of the CE 1226 Medieval tephra layer from the Reykjanes volcanic system, in Faculty of Earth Sciences. 2015, University of Iceland.
47. Alfano, F., et al., Reconstruction of total grain size distribution of the climactic phase of a long-lasting eruption: the example of the 2008–2013 Chaitén eruption. Bulletin of Volcanology, 2016. 78(7): p. 46.
48. Watt, S.F.L., et al., Fallout and distribution of volcanic ash over Argentina following the May 2008 explosive eruption of Chaitén, Chile. J. Geophys. Res., 2009. 114(B4): p. B04207.
49. Carn, S.A., et al., The Unexpected Awakening of Chaitén Volcano, Chile. Eos, Transactions American Geophysical Union, 2009. 90(24): p. 205-206.
50. Bonadonna, C. and A. Costa, Estimating the volume of tephra deposits: A new simple strategy. Geology, 2012. 40(5): p. 415-418.
51. Bonadonna, C. and B.F. Houghton, Total grain-size distribution and volume of tephra-fall deposits. Bulletin of Volcanology, 2005. 67(5): p. 441-456.

52. Prata, A.J. and I.F. Grant, Retrieval of microphysical and morphological properties of volcanic ash plumes from satellite data: Application to Mt Ruapehu, New Zealand. Quarterly Journal of the Royal Meteorological Society, 2001. 127(576): p. 2153-2179.
53. Gudnason, J., et al., The 1845 Hekla eruption: Grain-size characteristics of a tephra layer. Journal of Volcanology and Geothermal Research, 2018. 350: p. 33-46.
54. Scasso, R.A., H. Corbella, and P. Tiberi, Sedimentological analysis of the tephra from the 12–15 August 1991 eruption of Hudson volcano. Bulletin of Volcanology, 1994. 56(2): p. 121-132.
55. Kratzmann, D.J., et al., Simulations of tephra dispersal from the 1991 explosive eruptions of Hudson volcano, Chile. Journal of Volcanology and Geothermal Research, 2010. 190(3–4): p. 337-352.
56. Eychenne, J., et al., Causes and consequences of bimodal grain-size distribution of tephra fall deposited during the August 2006 Tungurahua eruption (Ecuador). Bulletin of Volcanology, 2012. 74(1): p. 187-205.
57. Eychenne, J., et al., Dynamics of explosive paroxysms at open-vent andesitic systems: High-resolution mass distribution analyses of the 2006 Tungurahua fall deposit (Ecuador). Earth and Planetary Science Letters, 2013. 361: p. 343-355.
58. Steffke, A.M., et al., Eruption chronologies, plume heights and eruption styles at Tungurahua Volcano: Integrating remote sensing techniques and infrasound. Journal of Volcanology and Geothermal Research, 2010. 193(3-4): p. 143-160.
59. Rose, W., et al., Nature and significance of small volume fall deposits at composite volcanoes: Insights from the October 14, 1974 Fuego eruption, Guatemala. Bulletin of Volcanology, 2008. 70(9): p. 1043-1067.
60. Bonadonna, C., et al., Tephra fallout in the eruption of Soufriere Hills Volcano, Montserrat. Geological Society, London, Memoirs, 2002. 21(1): p. 483-516.
61. Brazier, S., et al., Bimodal grain size distribution and secondary thickening in air-fall ash layers. Nature, 1983. 301: p. 115-119.
62. Buckland, H.M., et al., Sources of uncertainty in the Mazama isopachs and the implications for interpreting distal tephra deposits from large magnitude eruptions. Bulletin of Volcanology, 2020. 82(3): p. 23.
63. Gardner, J.E., S. Carey, and H. Sigurdsson, Plinian eruptions at Glacier Peak and Newberry volcanoes, United States: Implications for volcanic hazards in the Cascade Range. GSA Bulletin, 1998. 110(2): p. 173-187.
64. Engwell, S.L., R.S.J. Sparks, and S. Carey, Physical characteristics of tephra layers in the deep sea realm: the Campanian Ignimbrite eruption. Geological Society, London, Special Publications, 2014.
65. Perrotta, A. and C. Scarpati, Volume partition between the plinian and co-ignimbrite air fall deposits of the Campanian Ignimbrite eruption. Mineralogy and Petrology, 2003. 79(1): p. 67-78.
66. Rosi, M., et al., Plinian pumice fall deposit of the Campanian Ignimbrite eruption (Phlegraean Fields, Italy). Journal of Volcanology and Geothermal Research, 1999. 91(2): p. 179-198.
67. Kandlbauer, J., S.N. Carey, and R.S.J. Sparks, The 1815 Tambora ash fall: implications for transport and deposition of distal ash on land and in the deep sea. Bulletin of Volcanology, 2013. 75(4): p. 1-11.
68. Kandlbauer, J. and R.S.J. Sparks, New estimates of the 1815 Tambora eruption volume. Journal of Volcanology and Geothermal Research, 2014. 286: p. 93-100.
69. Rosi, M., et al., Fall vs flow activity during the 1991 climactic eruption of Pinatubo Volcano (Philippines). Bulletin of Volcanology, 2001. 62(8): p. 549-566.
70. Wiesner, M.G., et al., Grain size, areal thickness distribution and controls on sedimentation of the 1991 Mount Pinatubo tephra layer in the South China Sea. Bulletin of Volcanology, 2004. 66(3): p. 226-242.
71. Holasek, R.E., S. Self, and A.W. Woods, Satellite observations and interpretation of the 1991 Mount Pinatubo eruption plumes. Journal of Geophysical Research: Solid Earth, 1996. 101(B12): p. 27635-27655.
72. Bond, A. and R.S.J. Sparks, The Minoan eruption of Santorini, Greece. Journal of the geological society of London, 1976. 132: p. 1-16.
73. Sparks, R.S.J., et al., Sedimentology of the Minoan deep-sea tephra layer in the Aegean and eastern Mediterranean. Marine Geology, 1984. 54: p. 131-167.
74. Johnston, E., Tephra dispersal and volume of the Bronze age eruption of Santorini, in School of Earth Sciences. 2014, University of Bristol: Bristol. p. 405.
75. Pyle, D.M., New estimates for the volume of the Minoan eruption. Thera and the Aegean World III, 1990. 2: p. 113-121.
76. Eychenne, J., et al., Dynamics of an open basaltic magma system: the 2008 activity of the Halemaʻumaʻu Overlook vent, Kīlauea Caldera. Earth and Planetary Science Letters, 2015. 409: p. 19-60.
77. Durant, A.J., et al., Hydrometeor-enhanced tephra sedimentation: Constraints from the 18 May 1980 eruption of Mount St. Helens. Journal of Geophysical Research, 2009. 114(B3).
78. Sarna-Wojcicki, A., et al., Aeral distribution, thickness , mass, volume and grain size of air-fall ash from the six major eruptions of 1980. U.S. Geological Survey Professional Paper, 1981. 1250: p. 577-600.
79. Eychenne, J., et al., Impact of the lateral blast on the spatial pattern and grain size characteristics of the May 18, 1980 Mount St. Helens fallout deposit. Journal of Geophysical Research, 2015. 120: p. 6018-6038.
80. Sparks, R.S.J., J.G. Moore, and C.J. Rice, The initial giant umbrella cloud of the May 18th, 1980, explosive eruption of Mount St. Helens. Journal of Volcanology and Geothermal Research, 1986. 28: p. 257-274.
81. Carey, S., et al., Variations in column height and magma discharge during the May 18, 1980 eruption of Mount St Helens. Journal of Volcanology and Geothermal Research, 1990. 43: p. 99-112.